TECHNICAL NOTE

PARAMETRIC INSTABILITY OF AN ASYMMETRIC, ROTATING SANDWICH BEAM

P.R. Dash*, B.B. Maharathi**, R. Mallick*, B.B. Pani* and K. Ray+

Abstract

The parametric dynamic stability of an asymmetric, rotating sandwich beam and subjected to an axial pulsating load is investigated. A set of Hills equations are obtained from the non-dimensional equation of motion by the application of the general Galerkin method. The zones of parametric instability are obtained using Saito Otomi conditions. The influence of core-loss factor, geometric parameters and rotation parameters on the zones of instability are investigated.

Keywords*: parametric dynamic instability, rotating sandwich beam, zones of instability, simple and combination resonance zones*

Nomenclature

A_i (i=1,2,3)	= areas of cross section of a 3 layered beam, i = 1 for top layer
B	= width of beam
b	= distance of nearer end of the beam from the axis of rotation
$\overline{b}$	= b/l
c	= $h_1 + 2h_2 + h_3$
E_i (i=1,2,3)	= Youngs Modulli, i = 1 for top layer
$\ddot{f}_j$	= $\partial^2 f_j / \partial \overline{t}^2$
G_2	= in-phase shear modulus of the viscoelastic core
$\overset{*}{G}_2$	= G_2 (1+jη), complex shear modulus of core
$\overset{*}{g}$	= g (1+jη), complex shear parameter
g	= shear parameter
$2h_i$ (i=1,2,3)	= thickness of the ith layer i= 1 for top layer
h_{12}	= h_1/h_2
h_{31}	= h_3/h_1
I_i (i=1,2,3)	= second moments of area of cross section about a relevant axis, i = 1 for top layer
j	= $\sqrt{-1}$
l	= beam length
l_{h1}	= l/h_1
m	= mass/unit length of beam
$\overline{P}_l$	= non-dimensional amplitude for the dynamic loading
t	= time
$\overline{t}$	= non-dimensional time
$u_1(x,t)$, $U_1(x,t)$	= axial displacement at the middle of the top layer of beam
$w(x,t)$	= transverse deflection of beam
w'	= $\dfrac{\partial w}{\partial x}$
w''	= $\dfrac{\partial^2 w}{\partial x^2}$
$\overline{w}$	= $\dfrac{w}{l}$
$\ddot{\overline{w}}$	= $\dfrac{\partial^2 \overline{w}}{\partial \overline{t}^2}$

* Faculty, Department of Mechanical Engineering, University College of Engineering, Burla, Sambalpur-768 018, Orissa State, India, Email : prdash_india@yahoo.co.in
** Faculty, Indira Gandhi Institute of Technology (IGIT), Dehenkanal, Sarang-759 146, Orissa State, India
+ Faculty, Indian Institute of Technology Kharagpur, Kharagpur-721 302, India
Manuscript received on 04 Dec 2006; Paper reviewed, revised and accepted on 04 Aug 2008

$\overline{w}''$ $= \dfrac{\partial^2 \overline{w}}{\partial \overline{x}^2}$

t_o $= \sqrt{\dfrac{m l^4}{E_1 I_1 + E_3 I_3}}$

u_1' $= \dfrac{\partial u_1}{\partial x}$

$\overline{u}_1''$ $= \dfrac{\partial^2 \overline{u}_1}{\partial \overline{x}^2}$

f $= (l + b)^2$, for beam free $x = l$

$= \dfrac{l^3}{3} + b^2 + bl$at for all other cases

η = core-loss factor

λ_0 = rotation parameter

λ_1 = rotation parameter

$[\Phi]$ = a null matrix

$\overline{\omega}$ $= \omega t_0$

ω = frequency of forcing function

$\overline{\omega}$ = non-dimensional forcing frequency

Ω_0 = speeds of rotation

$\overline{\Omega}_0$ = non-dimensional rotation parameters

α $= \dfrac{E_1 A_1}{E_3 A_3}$

Introduction

Sandwich constructions with high strength facings and a light weight core have been very popular in aerospace applications. Typical sandwich members used varied from structural panels in aircraft to the helicopter rotor blades. In general high modulus and light weight characteristics of the sandwich construction normally have great advantages of high movability, power saving and high strength in robotics applications. Extensive publications have been available concerning the design and analysis of sandwich structure.

The dynamic behaviour of rotating beams is of great practical interest in the design of steam and gas turbine blades and helicopter blades. The vibrational behaviour of a rotating beam, oriented perpendicular to the axis of spin, was investigated by Bauer and Eidel [2]. It was observed that the speed of rotation has a very pronounced influence of the rotating beam and an increase in the speed of rotation may increase or decrease the natural frequencies depending on the boundary conditions. Abbas [5] studied the effect of rotational speed and root flexibilities on the first order simple resonance zones of a rotating Timoshenkos beam by using the finite element method. Bauchau and Hong [6] utilized the same method to analyze the effect of viscous damping on the response and stability of parametrically excited beams undergoing large deflections and rotations. Dynamic stability of an ordinary rotating beam with various boundary conditions was studied by Kar and Sujata [7]. The same authors [8] also studied the stability of a rotating, pre-twisted and pre-coned (which is shown in annexure) cantilever beam. Parametric instability of a rotating pre-twisted beam subjected to sinusoidal compressive axial loads was addressed by Tan et.al [9].

As it has been pointed out by many investigators the shear deformation of the core plays an important role in the flexural and dynamic behaviour of a sandwich beam, therefore, the flexural rigidity in the core and shear deformation of the facings were neglected in many analysis.

In the present study, the parametric instability of a rotating asymmetric sandwich beam with viscoelastic core and subjected to a pulsating axial load, is investigated as it has not been studied till now. The equations of motion for transverse vibrations of the beam are obtained using Hamiltons principle. The general Galerkin method is used to reduce the non-dimensional equations of motion to a set of coupled Hills equations [1] with complex coefficients. The regions of instability for simple and combination resonance are obtained by using the Saito-Otomi conditions [1]. The influence of core loss factor, geometric parameters and rotation parameters on the parametric resonance zones is investigated for the pinned-pinned and fixed-free boundary conditions.

Formulation of the Problem

A viscoelastic sandwich beam of length *l*, set-off at a distance b from the axis of rotation (z'-axis) and oriented along the *x*-axis, perpendicular to the axis of rotation is shown in Fig.1. The beam rotates about the vertical z'-axis at a constant angular velocity Ω_0 and is capable of oscillating in the *xz* plane. It is asymmetric with respect to the *xy* plane as layer 1 is not same as layer 3 both geometrically and materially. Note that some authors might call this a 'rotating column' configuration. However, it is also customary in the literature to call it a 'rotating beam'. This is followed throughout the paper.

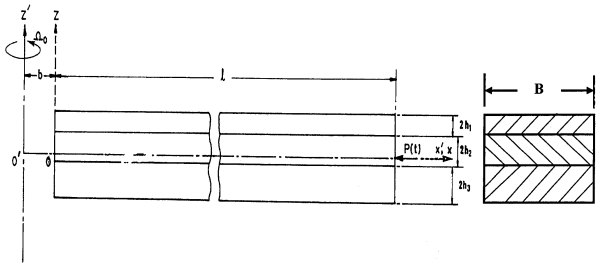

Fig.1 System configuration

The top layer of the beam is made of an elastic material of thickness $2h_1$ and Young modulus E_1 and the bottom layer is made of an elastic material of thickness $2h_3$ and Young modulus E_3. The core is made of a linearly viscoelastic material with a shear modulus $G_2^* = G_2 (1 + j\eta)$, where G_2 is the in-phase shear modulus, η is the core loss factor and $j = \sqrt{-1}$.

A pulsating axial load $P(t) = P_0 + P_1 \cos(\omega t)$ is applied at the end $x' = b+l$ of the beam. P_0 and P_1 are respectively the static and dynamic load amplitudes, ω is the frequency of the dynamic load and t is time.

The following assumption are made for deriving the equations of motion:

- The beam deflection w (x, t), parallel to z axis is small and is the same at all points of a given cross-section.
- The layers are perfectly bonded so that displacements are continuous across the interfaces. The elastic face layers obey the Euler-Bernoulli beam theory.
- The allowance for rotary inertia is neglected while calculating the kinetic energy of the system.
- Shear deformation of the facings are neglected.
- Damping in the viscoelastic core is predominantly due to shear. Bending and extensional effects in the core are neglected.
- The Kerwins assumption [10] is used.

According to the above assumption, $E_1 A_1 U_{1,x} + E_3 A_3 U_{3,x} = 0$

For the system

$$T = \frac{1}{2} m \int_0^l w_{1t}^2 \, dx + \frac{1}{2} m \Omega_0^2 \int_0^l \{(b+x) \int_0^x \left(\frac{\partial w}{\partial x}\right)^2 dx\} \, dx ,$$

$$V = \frac{1}{2} \int_0^l E_1 A_1 U_{1,x}^2 \, dx + \frac{1}{2} \int_0^l E_3 A_3 U_{3,x}^2 \, dx$$

$$+ \frac{1}{2} E_1 \int_0^l I_1 \left(\frac{\partial^2 w}{\partial x^2}\right)^2 dx + \frac{1}{2} E_3 \int_0^l I_3 \left(\frac{\partial^2 w}{\partial x^2}\right)^2 dx$$

$$+ \frac{1}{2} G_2^* \int_0^l A_2 v_2^2 \, dx + \frac{1}{2} m \Omega_0^2 \int_0^l \{(b+x) \int_0^x (\frac{\partial w}{\partial x})^2 dx\} dx$$

where $v_2 = \left(\frac{U_1 - U_3 - c\, w_{,x}}{2h_2}\right)$

Which is derived according to the Kerwin assumption.

Where T is the kinetic energy of the system. V strain energy of the system and W is the work done on the system by the external force.

Using Hamiltons principle

$\delta \int_{t_1}^{t_2} (T - V + W)\, dt = 0$. The equations of motion and the associated boundary conditions are obtained as follows :

$$\ddot{w} + (E_1 I_1 + E_3 I_3) \left[\frac{1}{m} + \frac{3\,\Omega_0^2}{2(E_1 A_1 + E_3 A_3)} \{f - (x+b)^2\}\right] w''$$

$$- 3 \frac{E_1 I_1 + E_3 I_3}{E_1 A_1 + E_3 A_3} \Omega_0^2 (x+b)\, w''$$

$$+ \left[-3 \frac{E_1 I_1 + E_3 I_3}{2 (E_1 A_1 + E_3 A_3)} \Omega_0^2 - \frac{1}{2} \Omega_0^2 \{f - (x+b)^2\} - \frac{G_2^* A_2 c^2}{m (2h_2)^2} + \frac{P(t)}{m}\right] w''$$

$$+ \frac{1}{2} \Omega_0^2 (x+b)\, w' + \frac{G_2^* A_2 c (1+\alpha)}{m (2h_2)^2} u_1' = 0 \qquad (1)$$

$$u_1'' - \frac{G_2^* A_2 (1+\alpha)}{(2h_2)^2 (E_1 A_1 + \alpha^2 E_3 A_3)} \{(1+\alpha) u_1 - c w'\} = 0 \qquad (2)$$

The boundary conditions at $x = 0$ and $x = \ell$ are :

$$w'' = 0 \quad \text{or} \quad w' = 0 \qquad (3)$$

$$(E_1 I_1 + E_3 I_3)\frac{\partial}{\partial x}\left[\left\{1+\frac{3\,m\,\Omega_0^2}{2(E_1 A_1 + E_3 A_3)}(f-(x+b)^2)\right\}w''\right]$$

$$-\left[\frac{m\,\Omega_0^2}{2}\left\{f-(x+b)^2\right\}+\frac{G_2^* A_2 c^2}{(2h_2)^2}+P(t)\right]w'$$

$$+\frac{G_2^* A_2 c(1+\alpha)}{(2h_2)^2}u_1 = 0 \quad \text{or,} \quad w = 0 \tag{4}$$

$$u_1' = 0 \quad \text{or} \quad u_1 = 0 \tag{5}$$

Introducing the non-dimensional variables $\bar{x} = x/l$, $\bar{w} = w/l$, $\bar{u}_1 = u_1/l$, and $\bar{t} = t/t_o$, where $t_o = \sqrt{\frac{m\,l^4}{E_1 I_1 + E_3 I_3}}$ and simplifying, the following non-dimensional equations of motion are obtained.

$$\ddot{\bar{w}} + \left[1+\frac{\lambda_0^2(1+E_{31}h_{31}^3)}{l_{h1}^2(1+E_{31}h_{31})}\left\{\frac{f}{l^2}-(\bar{x}+\bar{b})^2\right\}\right]\bar{w}'''' - \frac{2\lambda_0^2(1+E_{31}h_{31}^3)}{l_{h1}^2(1+E_{31}l_{31})}(\bar{x}+\bar{b})^2\bar{w}''''$$

$$+\left[-\frac{\lambda_0^2(1+E_{31}h_{31}^3)}{l_{h1}^2(1+E_{31}l_{31})}-\lambda_0^2\left\{\frac{f}{l^2}-(\bar{x}+\bar{b})^2\right\}-3g^*\left(1+\frac{h_{12}+h_{32}}{2}\right)^2+\bar{P}(t)\right]\bar{w}''$$

$$+\lambda_0^2(\bar{x}+\bar{b})\bar{w}'+\frac{3}{2}g^* l_{h1} h_{12}\left(1+\frac{h_{12}+h_{32}}{2}\right)(1+\alpha)\bar{u}_1' = 0 \tag{6}$$

$$\bar{u}_1'' - \frac{g^*}{4}h_{12}^2\frac{1+E_{31}h_{31}^3}{1+\alpha^2 E_{31}h_{31}}(1+\alpha)\left[\left(1+\alpha\right)\bar{u}_1 - \left(2\left(1+\frac{h_{12}+h_{32}}{2}\right)/(l_{h1}h_{12})\right)\bar{w}'\right] = 0 \tag{7}$$

The associated non-dimensional boundary conditions at $\bar{x} = 0$ and $\bar{x} = 1$ are :

$$\bar{w}'' = 0 \quad \text{or} \quad \bar{w}' = 0 \tag{8}$$

$$\frac{\partial}{\partial x}\left[\left(1+\lambda_1^2\left\{\frac{f}{l^2}-(\bar{x}+\bar{b})^2\right\}\right)\bar{w}''\right]$$

$$-\left[\lambda_0^2\left\{\frac{f}{l^2}-(\bar{x}+\bar{b})^2\right\}\bar{w}'-3g^*\left(1+\frac{h_{12}+h_{32}}{2}\right)^2+\bar{P}(t)\right]\bar{w}'$$

$$+\frac{3}{2}g^* l_{h1} h_{12}(1+\alpha)\left(1+\frac{h_{12}+h_{32}}{2}\right)\bar{u}_1' = 0$$

$$\text{or } \bar{w} = 0 \tag{9}$$

$$\bar{u}_1' = 0 \quad \text{or} \quad \bar{u}_1 = 0 \tag{10}$$

The various parameters etc. are defined as :

$E_{31} = E_3/E_1$, $h_{31} = h_3/h_1$, $l_{h1} = l/h_1$, $h_{12} = h_1/h_2$, $g^* = g(1+j\eta) = \dfrac{G_2^* h_{21} l_{h1}^2}{E_1(1+E_{31}h_{31}^3)}$

g being the shear parameter

$$\lambda_0 = \sqrt{\frac{m\,\Omega_0^2 l^4}{2(E_1 I_1 + E_3 I_3)}}$$

$$\lambda_1 = \sqrt{\left(\frac{3\,m\,\Omega_0^2 l^2}{2(E_1 A_1 + E_3 A_3)}\right)}$$

are rotation parameters.

$$\bar{P}(t) = \bar{P}_0 + \bar{P}_1\cos(\bar{\omega}\bar{t}), = \frac{(P(t)\,l^2)}{(E_1 I_1 + E_3 I_3)}$$

is the non-dimensional load.

Approximate Solution

Approximate solution to the non-dimensional equations of motion are assumed as

$$\bar{w}(\bar{x},\bar{t}) = \sum_{i=1}^{i=N} f_i(\bar{t})\, w_i(\bar{x}) \tag{11}$$

$$\bar{u}_1(\bar{x},\bar{t}) = \sum_{k=N+1}^{k=2N} f_k(\bar{t})\, u_{1k}(\bar{x}) \tag{12}$$

where f_r (r = 1,2, ..., 2N) are the generalized coordinates and w_i and u_{1k} are the coordinate functions satisfying as many boundary conditions as possible [4]. For the pinned-pinned case, the shape functions chosen are

$$w_i(\bar{x}) = \sin(i\pi\bar{x})$$

$$u_{ik}(\bar{x}) = \cos(\bar{k}\pi\bar{x}), \quad \bar{k} = k - N$$

For i = 1,2 ....., N and k = N+1, N+2, ..., 2N.

For the clamped-free case, the approximating functions are

$$w_i(\bar{x}) = (i+2)(i+3)\bar{x}^{i+1} - 2i(i+3)\bar{x}^{i+2} + i(i+1)\bar{x}^{i+2}$$

$$u_{1k}(\bar{x}) = \bar{x}^{\bar{k}} - \left[\bar{k}/(\bar{k}+1)\right]\bar{x}^{\bar{k}+1}$$

Substitution of the series solutions in the non-dimensional equations of motion and subsequent application of the general Galerkin method [4] leads to the following matrix equations of motion.

$$[m]\{\ddot{f}_j\} + \left[k_{11}\right]\{f_j\} + \left[k_{12}\right]\{f_l\} = \{0\} \tag{13}$$

$$\left[k_{22}\right]\{f_l\} + \left[k_{21}\right]\{f_j\} = \{0\} \tag{14}$$

where j = 1,2, ..., N and l = N+1, ..., 2N. The various matrix elements are given by

$$m_{ij} = \int_0^1 w_i w_j \, d\bar{x}$$

$$k_{11ij} = \int_0^1 \left[1 + \lambda_1\left\{\frac{f}{l^2} - (\bar{x}+\bar{b})^2\right\}\right] w_i'' w_j'' \, d\bar{x}$$

$$+ \lambda_0^2 \int_0^1 \left\{\frac{f}{l^2} - (\bar{x}+\bar{b})^2\right\} w_i' w_j' \, d\bar{x}$$

$$+ \left\{3g^*\left(1 + \frac{h_{12}+h_{32}}{2}\right)^2 - \bar{P}(\bar{t})\right\}\left(\int_0^1 w_i' w_j' \, d\bar{x}\right)$$

$$k_{12jl} = -(3/2)\, g^*\, l_{h1}\, h_{12}(1+\alpha)$$

$$\left(1 + \frac{h_{12}+h_{32}}{2}\right)\left(\int_0^1 u_{1l} w_i' \, d\bar{x}\right)$$

$$k_{21li} = -(3/2)\, g^*\, l_{h1}\, h_{12}(1+\alpha)$$

$$\left(1 + \frac{h_{12}+h_{32}}{2}\right)\left(\int_0^1 u_{1l} w_i' \, d\bar{x}\right)$$

$$k_{22kl} = 3\, l_{h1}^2 \frac{(1+\alpha^2 E_{31} h_{31})}{(1+E_{31} h_{31}^3)}\left(\int_0^1 u_{1k}' u_{1l}' \, d\bar{x}\right)$$

$$+ (3/4)\, g^*\, l_{h1}^2 h_{12}^2 (1+\alpha)^2 \left(\int_0^1 u_{1k} u_{1l} \, d\bar{x}\right)$$

From Eq.(14) $\{f_l\} = -\left[k_{22}\right]^{-1}\left[k_{21}\right]\{f_j\}$ (15)

where

$$[k_{21}] = [k_{12}]^T \tag{16}$$

Substitutionof above in Eq. (13) and subsequent simplification leads to

$$[m]\{\ddot{f}_j\} + \left[[k] - \bar{P}_0[H]\right]\{f_j\} - \bar{P}_1 \cos(\bar{\omega}\bar{t})[H]\{f_j\} = \{0\} \tag{17}$$

where

$$[k] = [\bar{k}] - [k_{12}][k_{22}]^{-1}[k_{12}]^T$$

$$\bar{k}_{ij} = \int_0^1 \left[1 + \lambda_1\left\{\frac{f}{l^2} - (\bar{x}+\bar{b})^2\right\}\right] w_i'' w_j'' \, d\bar{x}$$

$$+ \lambda_0^2 \int_0^1 \left\{\frac{f}{l^2} - (\bar{x}+\bar{b})^2\right\} w_i' w_j' \, d\bar{x}$$

$$+ 3\, g^* \left(1 + \frac{h_{12}+h_{32}}{2}\right)^2 \int_0^1 w_i' w_j' \, d\bar{x}$$

$$H_{ij} = \int_0^1 w_i' w_j' \, d\bar{x}$$

Regions of Instability

Let [L] be a modal matrix of $[m]^{-1}\left[[k] - \bar{P}_0 [H]\right]$. Introducing the linear transformation $\{f_j\} = [L]\{u\}$, where $\{u\}$ is a new set of generalized co-ordinates, Eq. (17) reduces to a system of N coupled Hill's Equations with complex coefficients.

$$\{\ddot{u}_n\} + \left[\omega_n^2\right]\{u_n\} + \bar{P}_1 \cos\bar{\omega}\bar{t}\ [B]\{u_n\} = \{0\},$$

$$\text{here } \bar{P}_1 = \frac{P_1 l^2}{E_1 I_1 + E_3 I_3} \tag{18}$$

where ω_n^2 are the distinct eigenvalues of $[m]^{-1}\left[[k] - \bar{P}_0 [H]\right]$ and are given by

$$\left[\omega_n^2\right] = \begin{bmatrix} \omega_1^2 & 0 & .. & .. & 0 \\ 0 & \omega_2^2 & .. & .. & 0 \\ .. & .. & .. & .. & .. \\ 0 & 0 & .. & .. & \omega_N^2 \end{bmatrix}$$

and $[B] = -[L]^{-1}[m]^{-1}[H][L]$

The above equation can be written as :

$$\ddot{u}_n + \omega_n^2 u_n + \bar{P}_1 \cos\bar{\omega}\bar{t} \sum_{m=1}^{N} b_{nm} u_n = 0, \quad n = 1, 2 \ldots N \tag{19}$$

where the complex quantities w_n and b_{nm} are given by

$$\omega_n = \omega_{n,R} + j\,\omega_{n,1}$$

$$b_{nm} = b_{nm,R} + j b_{nm,1}$$

The boundary of the regions of instability for simple and combination resonances are obtained using the Saito-Otomi conditions [1].

Case (A) : Simple Resonance

In this case, the resions of instability are given by

$$\left|\frac{\bar{\omega}}{2} - \omega_{\mu,R}\right| < \frac{1}{4}\sqrt{\frac{\bar{P}_1^2 (b_{\mu\mu,R}^2 + b_{\mu\mu,l}^2)}{\omega_{\mu,R}} - 16\,\omega_{\mu,l}^2}$$

when damping is present and

$$\left|\frac{\bar{\omega}}{2} - \omega_{\mu,R}\right| < \frac{1}{4}\,\frac{\left|\bar{P}_1 b_{\mu\mu,R}\right|}{\omega_{\mu,R}}$$

for the undamped case and for m = 1, 2, ..., N.

Case (B) : Combination Resonance of the Sum Type

This type of resonance occurs when $\mu \neq \nu$; μ, ν = 1, 2 .... N and the regions of instability are given by :

$$\left|\frac{\bar{\omega}}{2} - \frac{1}{2}(\omega_{\mu,R} + \omega_{\nu,R})\right|$$

$$< \frac{\omega_{\mu,I} + \omega_{\nu,I}}{8\sqrt{(\omega_{\mu,I} + \omega_{\nu,I})}}$$

$$\sqrt{\frac{\bar{P}_1^2}{\omega_{\mu,R}\omega_{\nu,R}}(b_{\mu\nu,R}\, b_{\nu\mu,R} + b_{\mu\nu,I}\, b_{\nu\mu,I}) - 16\omega_{\mu,I}\omega_{\nu,I}}$$

for the damped case and

$$\left|\frac{\bar{\omega}}{2} - \frac{1}{2}(\omega_{\mu,R} + \omega_{\nu,R})\right| < \frac{\bar{P}_1}{4}\sqrt{\frac{b_{\mu\nu,R}\, b_{\nu\mu,R}}{\omega_{\mu,R}\,\omega_{\nu,R}}}$$

for the undamped case.

Case (C) : Combination Resonance of Different Type

This type of resonance occurs when $\mu < \nu$, (μ, ν = 1, 2 .... N) and the regions of instability are given by

$$\left|\frac{\bar{\omega}}{2} - \frac{1}{2}(\omega_{\nu,R} - \omega_{\mu,R})\right|$$

$$< \frac{\omega_{\mu,I} + \omega_{\nu,I}}{8\sqrt{(\omega_{\mu,I} + \omega_{\nu,I})}}$$

$$\sqrt{\frac{\bar{P}_1^2}{\omega_{\mu,R}\,\omega_{\nu,R}}(-b_{\mu\nu,R}\,b_{\nu\mu,R}+b_{\mu\nu,I}\,b_{\nu\mu,I})-16\omega_{\mu,I}\,\omega_{\nu,I}}$$

for the damped case and

$$\left|\frac{\bar{\omega}}{2}-\frac{1}{2}(\omega_{\nu,R}-\omega_{\mu,R})\right|<\frac{\bar{P}_1}{4}\sqrt{\frac{-b_{\mu\nu,R}\,b_{\nu\mu,R}}{\omega_{\mu,R}\,\omega_{\nu,R}}}$$

for the damped case and

Numerical Results and Discussion

Numerical results were obtained for various values of the core loss factor η, the non-dimensional geometric parameters, h_{31}, h_{12}, l_{h1}, $\bar{b}$, the modulli ratio G_2/E_1, the rotational parameters λ_0, λ_1 and the shear parameter *g*. For relevant values of the parameters, the results of the present study were compared and found to be in good agreement with [7]. The following values of parameters are used, unless otherwise stated : η = 0.05, h_{31} = h_{12} = 1.0, l_{h1} = 40, b = 0.05, G_2/E_1 = 0.001, g = 0.1, λ_0 = 0.05 and λ_1 = 01.

Figures 2.1(a, b) to Fig. 2.28(a, b) depict the zones of parametric resonance for studying the effects of non-dimensional parameters on parametric instability of the system. In these plots, $\omega_{q,R}$ is placed by ω_q (q = 1,2,3,4) for brevity.

Figures 2.1(a, b) to Fig. 2.3(a, b) show the effect of core loss factor η upon the regions of instability. With the introduction as well as an increase of core damping, stability is seen to improve. The instability zones simply move up without appreciable sideways shift. The combination resonance zones for the clamped-free case mostly disappear as n increases to 0.5. The areas of all the unstable zones decrease, giving rise to an improvement is stability.

Figures 2.4(a, b) to Fig. 2.7(a,b) in conjuction with Fig.2.2(a,b) study the effect of h_{12} on parametric stability. At low values of h_{12}, with an increase in this parameter, the zones mostly move downwards as well as towards left, except the zone near $\omega_4 + \omega_3$ in Fig.2.5(b) for the clamped-free case. This indicates an overall worsening of stability, since the area of the unstable zones increase as well as crowd in the low excitation frequency zone. However, for the higher values of h_{12}, the zones mostly move up and towards higher value of $\bar{\omega}$. There is a decrease in the zone areas and this effect is more pronounced for the simple resonance zones. Overall stability is seen to improve. Thus, in this case, stability improves or worsens depending on the value of h_{12}.

It is apparent from Figs.2.8(a, b) to Fig.2.10(a, b), that with an increase in l_{h1}, the unstable zones move-up as well as shift to the right, thereby improving the stability of the system.

Figures 2.11(a, b) to Fig. 2.13(a, b) depict the dependence of parametric instability on $\bar{b}$. An increase in its value shows that the simple resonance zones remains almost unaffected. However, for the clamped-free case, the combination resonance zones considerably broaden as well as move down to some extent. For the pinned-pinned case, combination resonance zones appear. Thus, system stability is worsened.

A study of Figs. 2.14(a, b) to Fig. 2.16(a, b) reveals that G_2/E_1, considerably improves parametric stability of the system with an increase in its value, all the zones move to higher excitation frequency regions and they also move up. Some zones even disappear.

The effect of the rotation parameter λ_1 is considered in Figs. 2.17(a, b) to Fig.2.20(a, b). For low values of this parameter, the resonance zones remains almost unaffected by an increase in its value. Raising λ_1 above 0.1 leads to the appearance of a narrow band of combination resonance zones for the pinned-pinned case and thus deteriorates stability. For the clamped-free case, the combination resonance zones near $\omega_2 + \omega_1$, $\omega_3 + \omega_1$ and $\omega_3 + \omega_2$ broaden considerably and move downward, thereby worsening stability. However, the zones near $\omega_4 + \omega_1$, $\omega_4 + \omega_2$ and $\omega_4 + \omega_3$ move towards right and also move-up, thereby improving stability to some extent for higher values of $\bar{\omega}$.

Figures 2.21(a, b) to Fig.2.23(a, b) show the dependence of the shear parameter *g* on parametric stability of the system. An increase in *g* not only shifts the zones upward, it also shifts them to higher excitation frequency zones, thereby improving stability over the range considered.

The influence of λ_0 on dynamic stability can be seen from Figs. 2.4(a, b) to Fig. 2.26(a, b). An increase in its value shifts the zones to the right and also move them up. This effect is more pronounced for the zones in the lower excitation frequency zone. Thus, λ_0 improves stability.

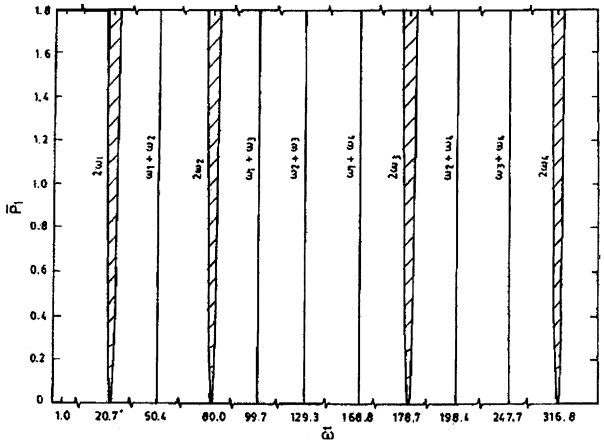

Fig.2.1 (a) Effect of η *on zones of instability :* η = *0*

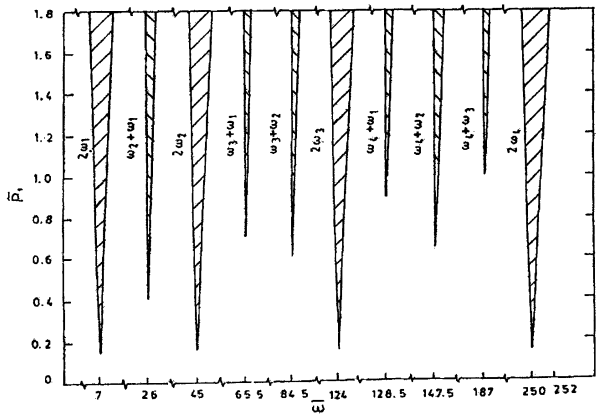

Fig.2.2 (b) Effect of η *on zones of instability :* η = *0.05*

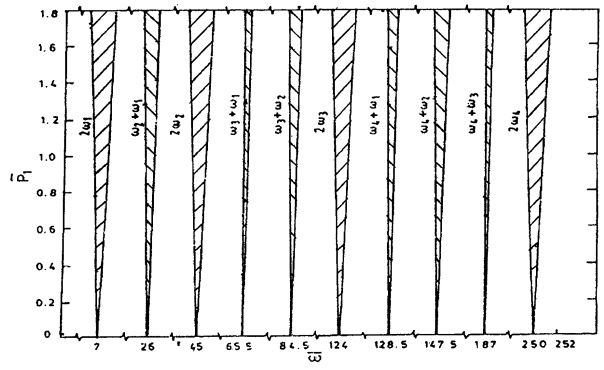

Fig.2.1 (b) Effect of η *on zones of instability :* η = *0*

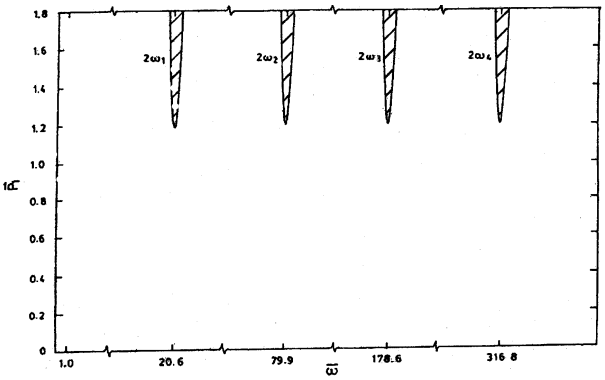

Fig.2.3 (a) Effect of η *on zones of instability :* η = *0.5*

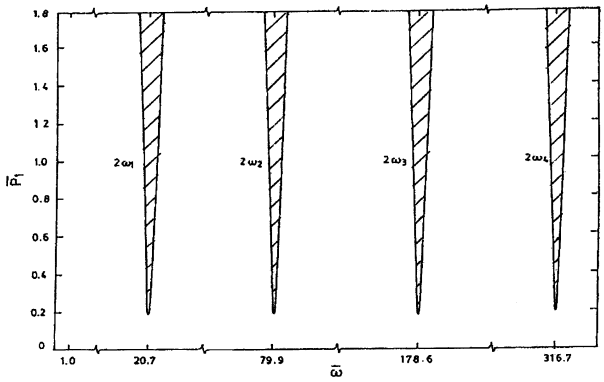

Fig.2.2 (a) Effect of η *on zones of instability :* η = *0.05*

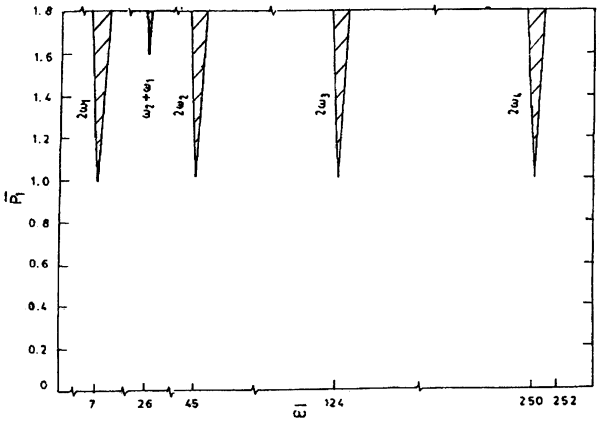

Fig.2.3 (b) Effect of η *on zones of instability :* η = *0.5*

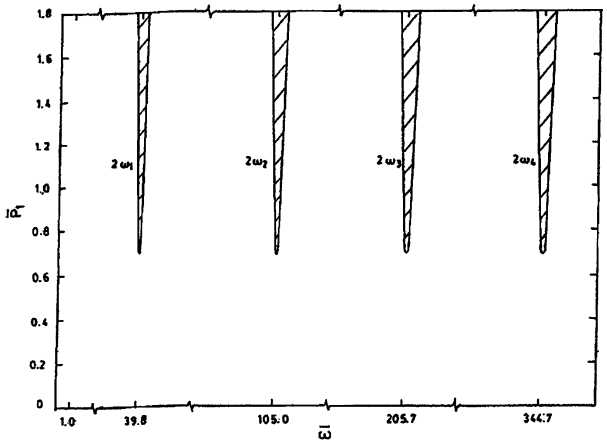

Fig.2.4 (a) Effect of h_{12} on zones of instability : h_{12} = 0.01

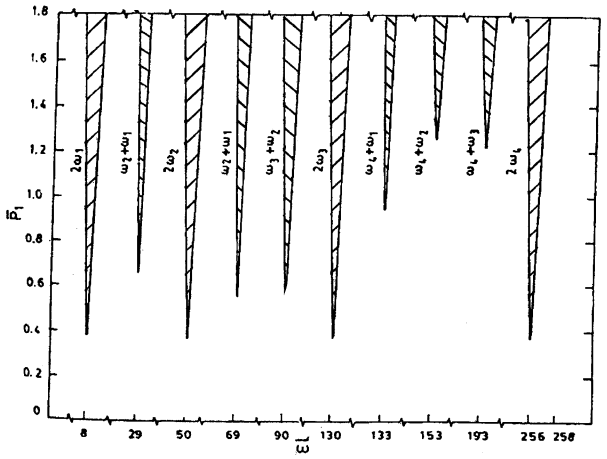

Fig.2.5 (b) Effect of h_{12} on zones of instability : h_{12} = 0.1

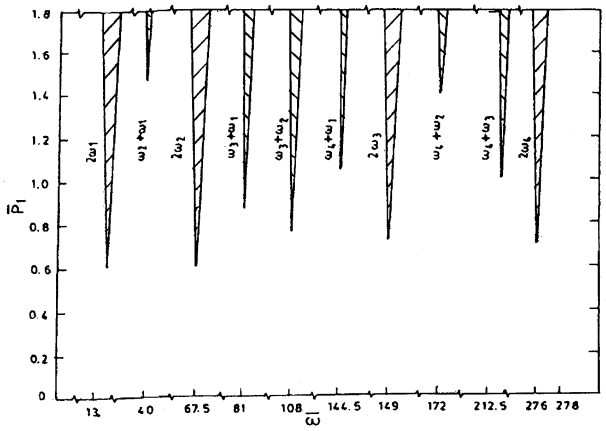

Fig.2.4 (b) Effect of h_{12} on zones of instability : h_{12} = 0.01

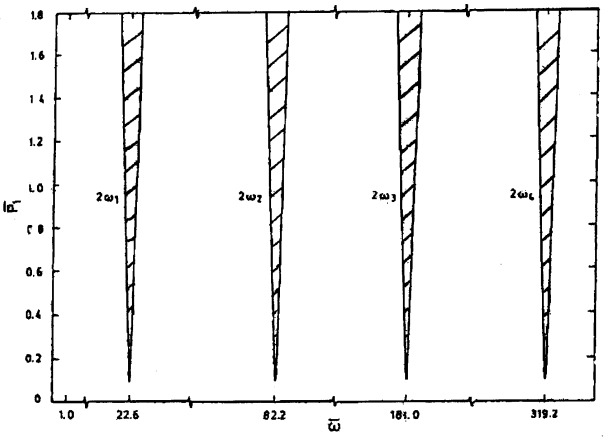

Fig.2.6 (a) Effect of h_{12} on zones of instability : h_{12} = 10

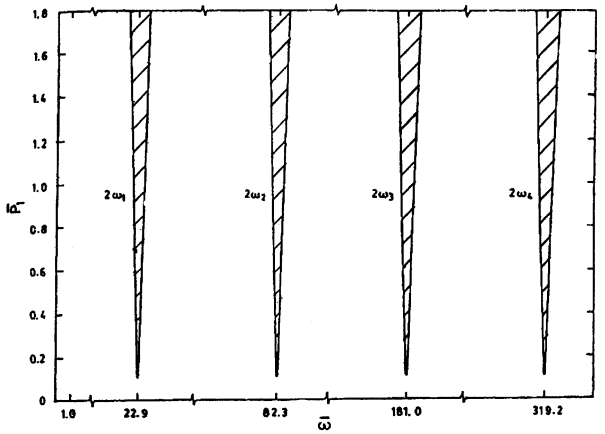

Fig.2.5 (a) Effect of h_{12} on zones of instability : h_{12} = 0.1

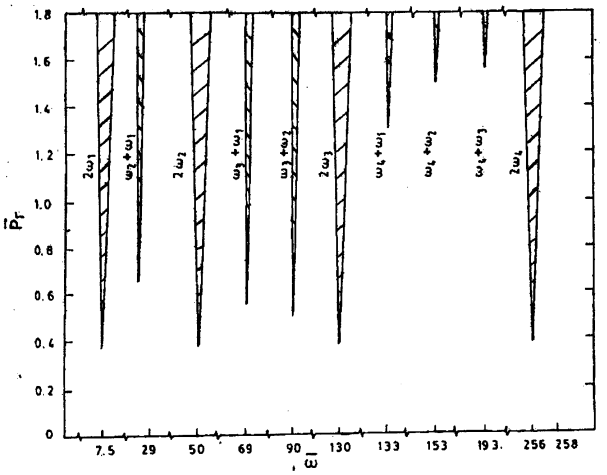

Fig.2.6 (b) Effect of h_{12} on zones of instability : h_{12} = 10

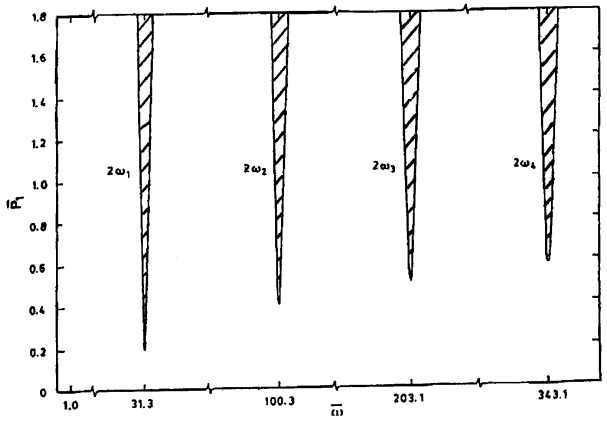

Fig.2.7 (a) Effect of h_{12} on zones of instability : h_{12} = 100

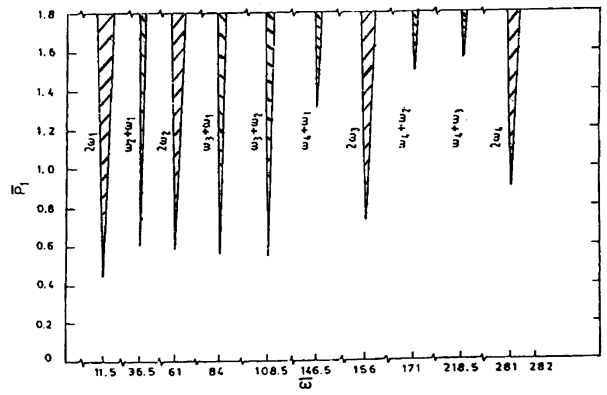

Fig.2.7 (b) Effect of h_{12} on zones of instability : h_{12} = 100

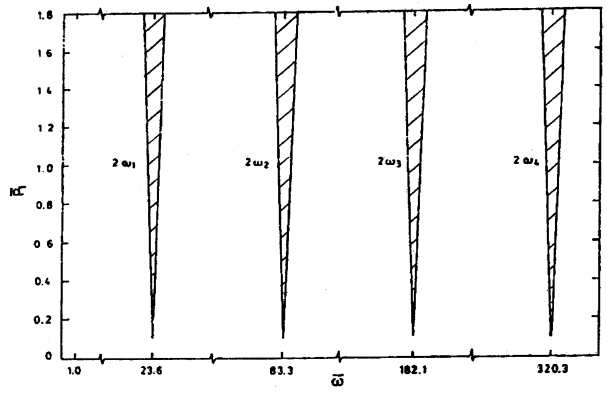

Fig.2.8 (a) Effect of l_{h1} on zones of instability l_{h1} = 50

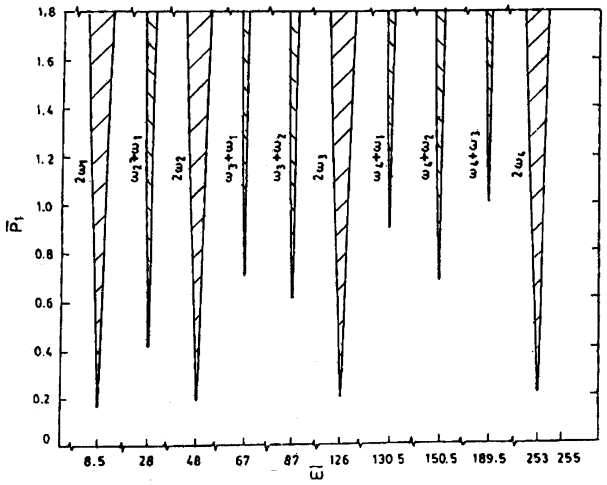

Fig.2.8 (b) Effect of l_{h1} on zones of instability: l_{h1} = 50

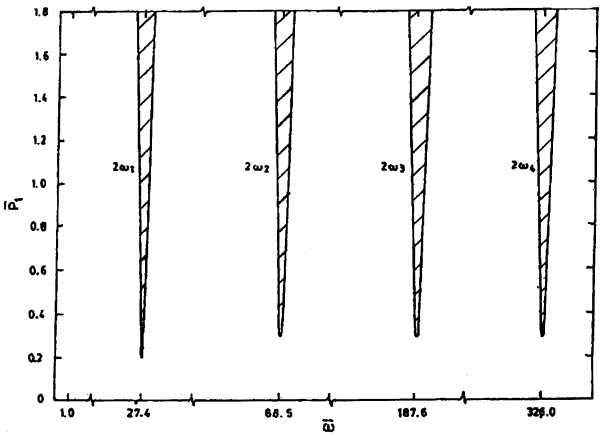

Fig.2.9 (a) Effect of l_{h1} on zones of instability: l_{h1} = 75

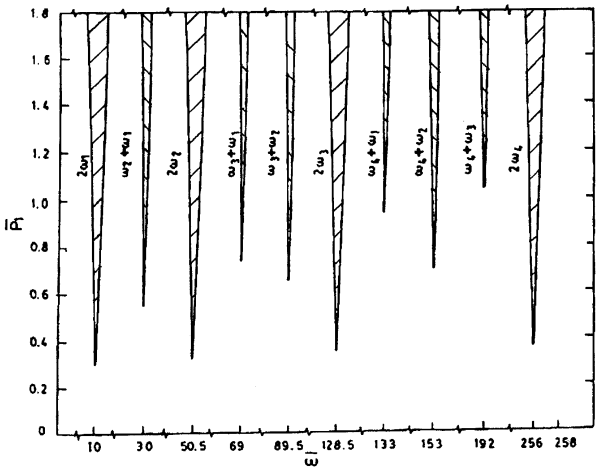

Fig.2.9 (b) Effect of l_{h1} on zones of instability: l_{h1} = 75

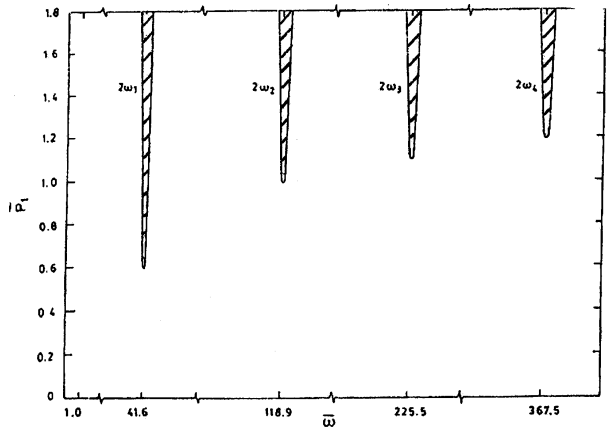

Fig.2.10 (a) Effect of l_{h1} on zones of instability: l_{h1} = 100

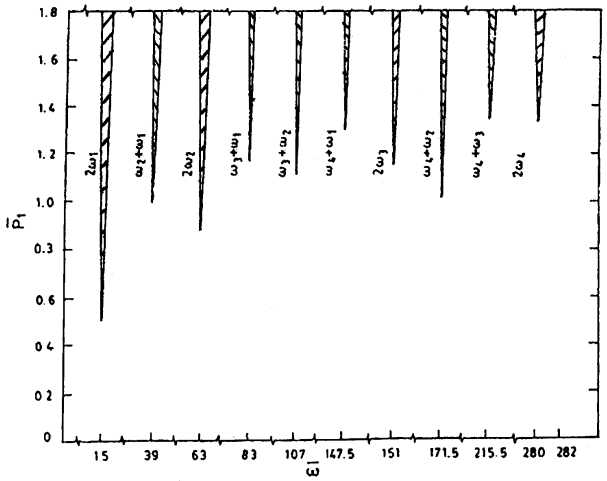

Fig.2.10 (b) Effect of l_{h1} on zones of instability: l_{h1} = 100

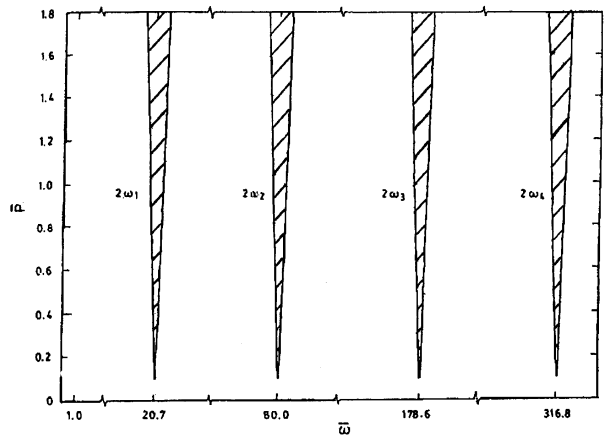

Fig.2.11 (a) Effect of $\bar{b}$ on zones of instability: $\bar{b}$ = 0.05

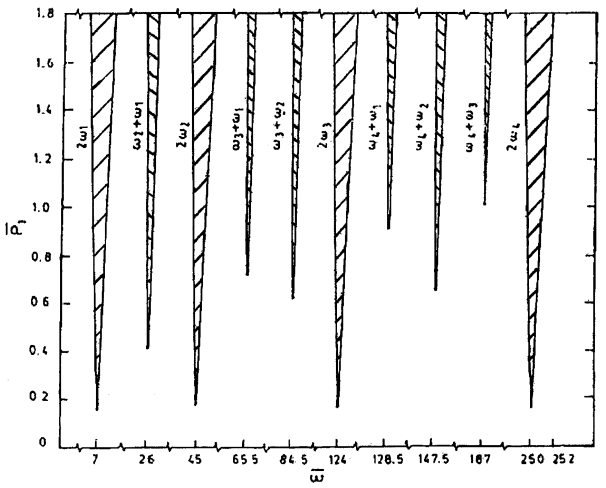

Fig.2.11 (b) Effect of $\bar{b}$ on zones of instability: $\bar{b}$ = 0.05

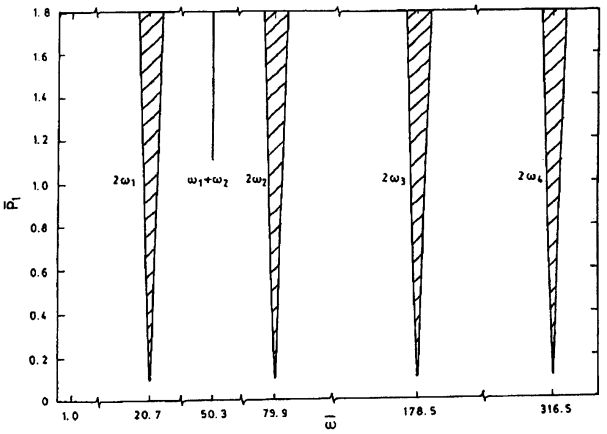

Fig.2.12 (a) Effect of $\bar{b}$ on zones of instability: $\bar{b}$ = 0.5

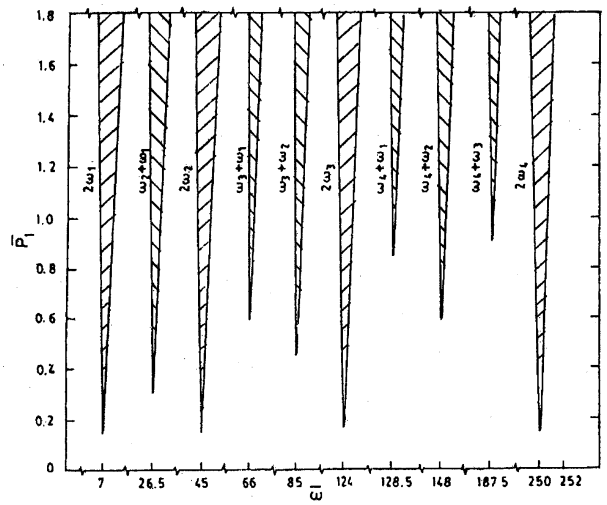

Fig.2.12 (b) Effect of $\bar{b}$ on zones of instability: $\bar{b}$ = 0.5

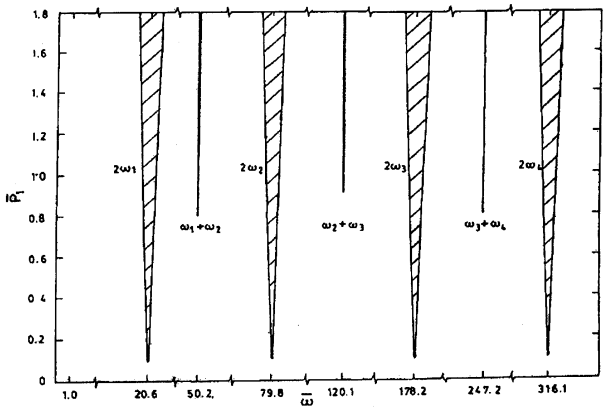

Fig.2.13 (a) Effect of $\bar{b}$ on zones of instability: $\bar{b}$ = 1.0

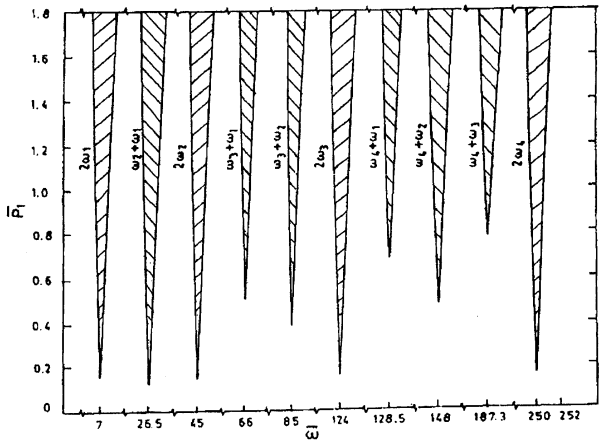

Fig.2.13 (b) Effect of $\bar{b}$ on zones of instability: $\bar{b}$ = 1.0

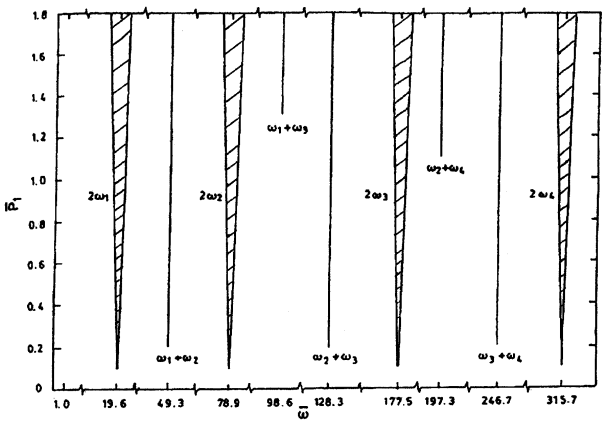

Fig.2.14 (a) Effect of G_2/E_1 on zones of instability: G_2/E_1 = 0.0001

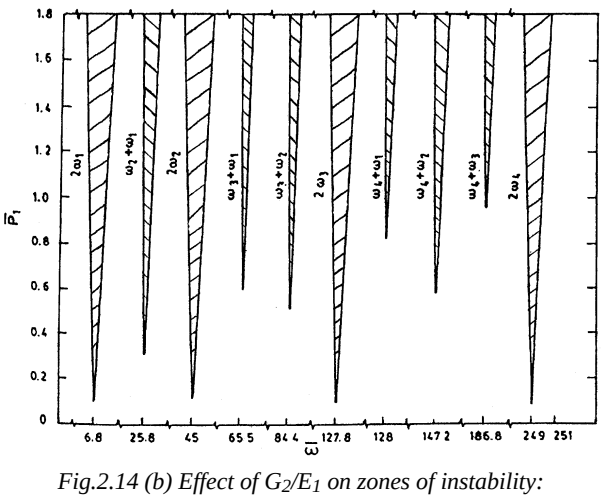

Fig.2.14 (b) Effect of G_2/E_1 on zones of instability: G_2/E_1 = 0.0001

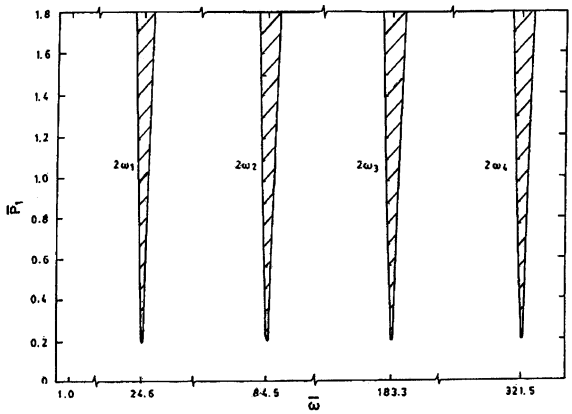

Fig.2.15 (a) Effect of G_2/E_1 on zones of instability: G_2/E_1 = 0.005

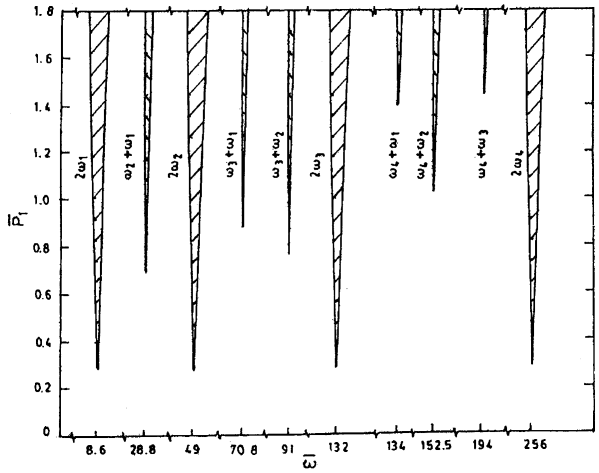

Fig.2.15 (b) Effect of G_2/E_1 on zones of instability: G_2/E_1 = 0.005

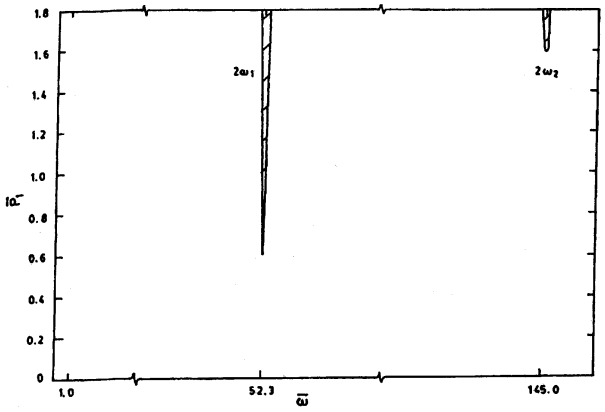

Fig.2.16 (a) Effect of G_2/E_1 on zones of instability: $G_2/E_1 = 0.1$

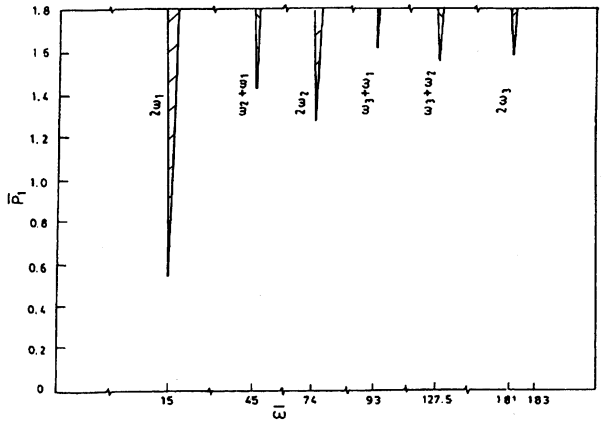

Fig.2.16 (b) Effect of G_2/E_1 on zones of instability: $G_2/E_1 = 0.1$

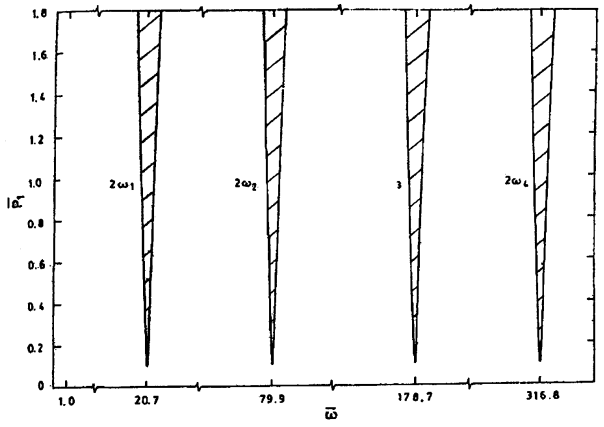

Fig.2.17 (a) Effect of λ_1 on zones of instability: $\lambda_1 = 0.001$

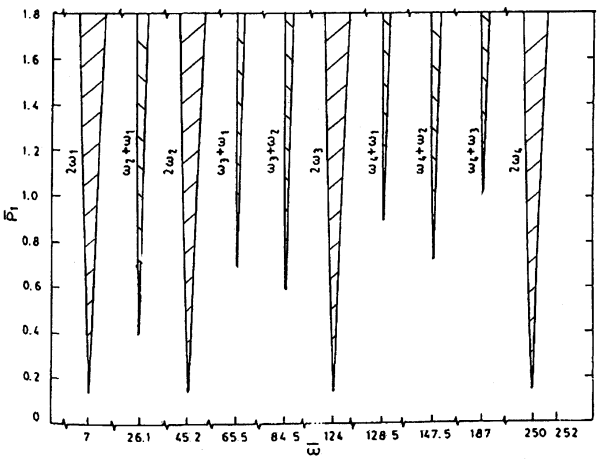

Fig.2.17 (b) Effect of λ_1 on zones of instability: $\lambda_1 = 0.001$

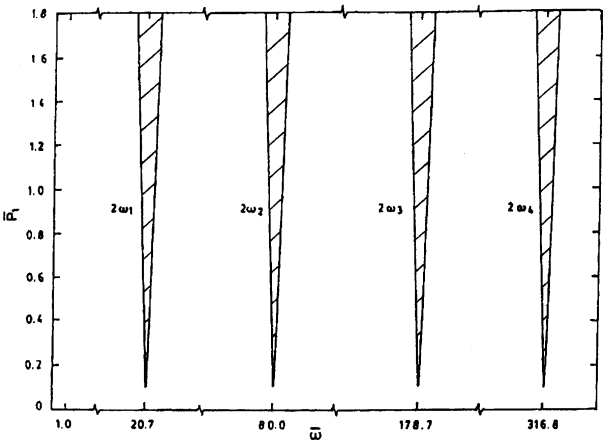

Fig.2.18 (a) Effect of λ_1 on zones of instability: $\lambda_1 = 0.01$

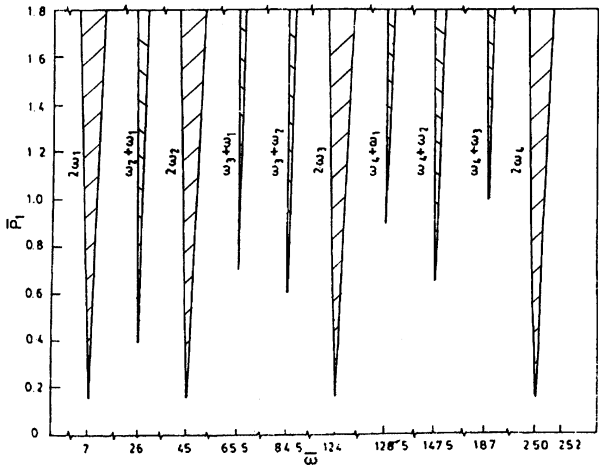

Fig.2.18 (b) Effect of λ_1 on zones of instability: $\lambda_1 = 0.01$

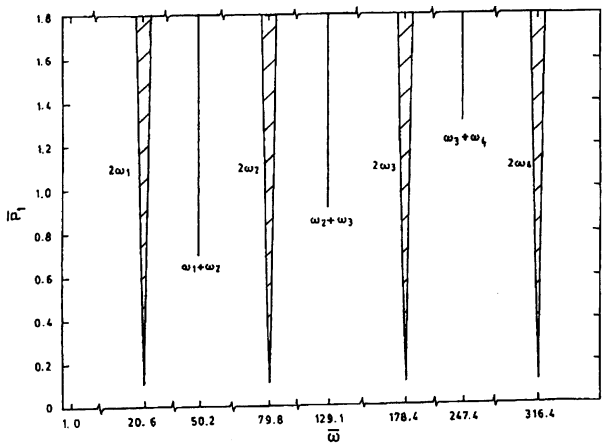

Fig.2.19 (a) Effect of λ_1 on zones of instability: $\lambda_1 = 0.02$

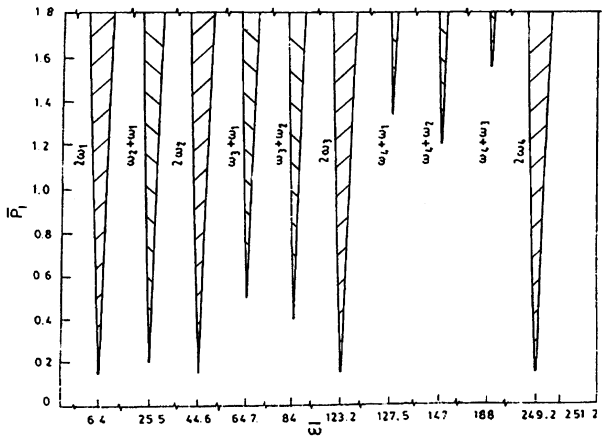

Fig.2.19 (b) Effect of λ_1 on zones of instability: $\lambda_1 = 0.02$

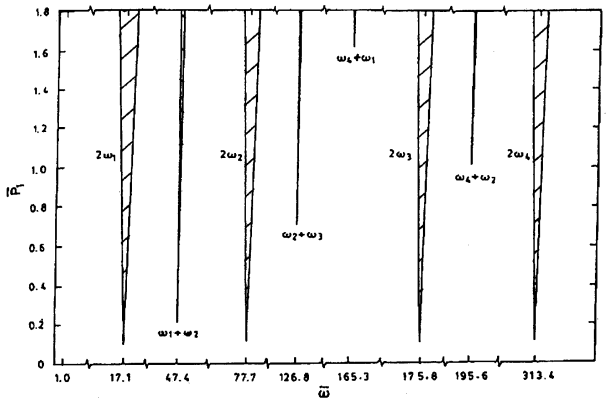

Fig.2.20 (a) Effect of λ_1 on zones of instability: $\lambda_1 = 0.5$

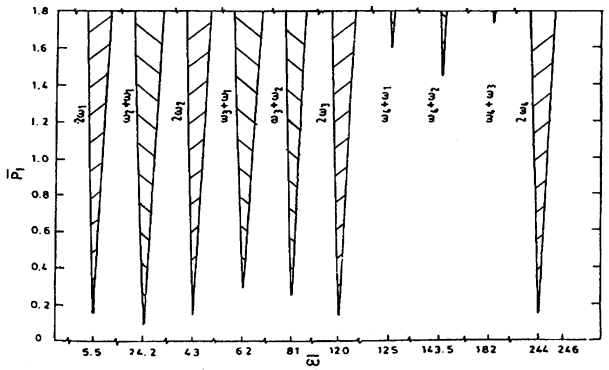

Fig.2.20 (b) Effect of λ_1 on zones of instability: $\lambda_1 = 0.5$

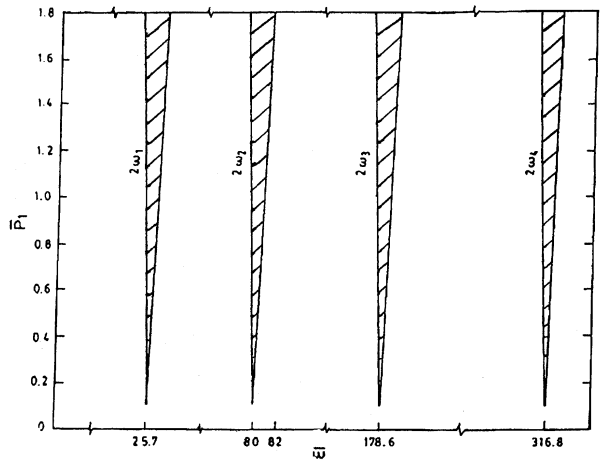

Fig.2.21 (a) Effect of g on zones of instability: g = 0.1

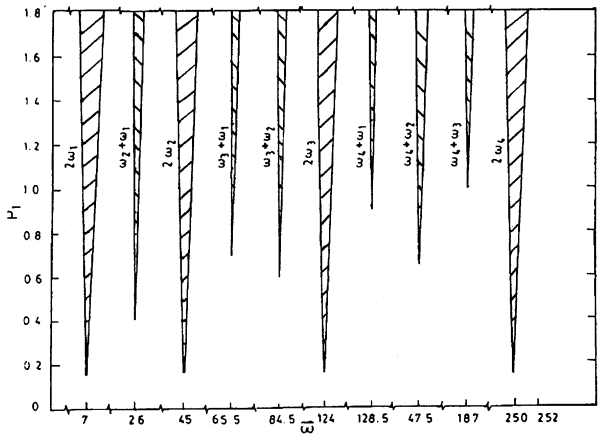

Fig.2.21 (b) Effect of g on zones of instability: g = 0.1

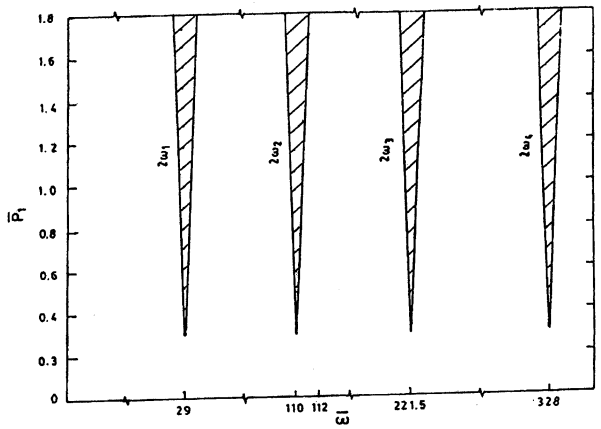

Fig.2.22 (a) Effect of g on zones of instability: g = 1.0

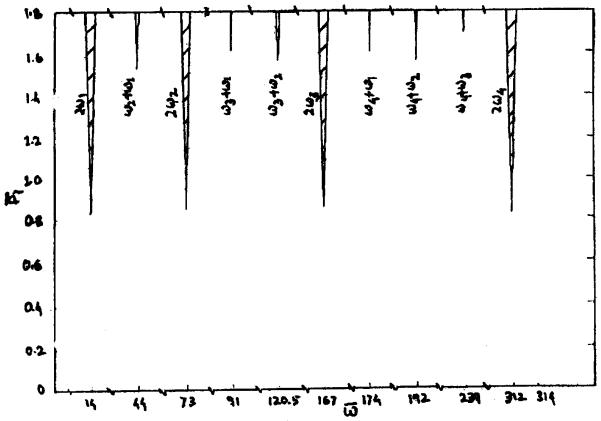

Fig.2.23 (b) Effect of g on zones of instability: g = 10

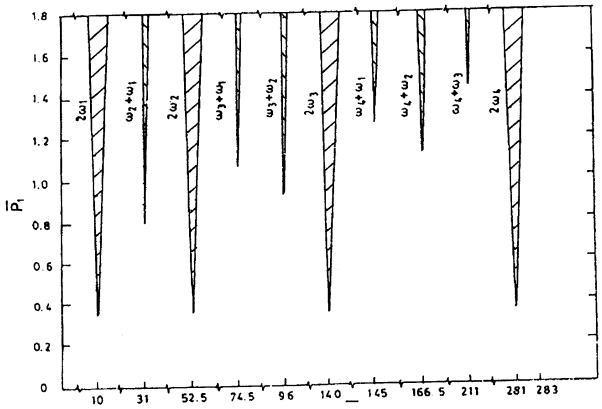

Fig.2.22 (b) Effect of g on zones of instability: g = 1.0

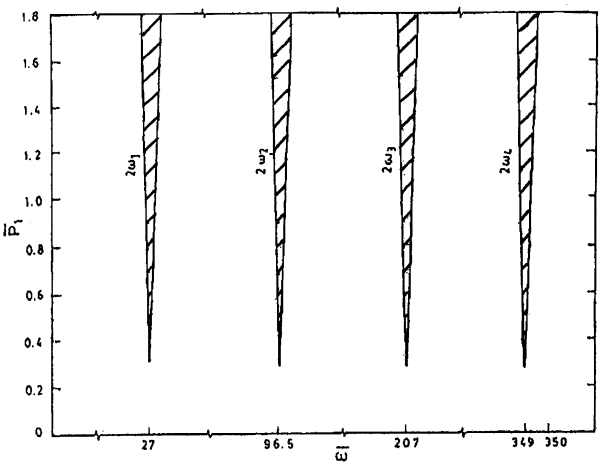

Fig.2.24 (a) Effect of λ_0 on zones of instability: λ_0 = 0.1

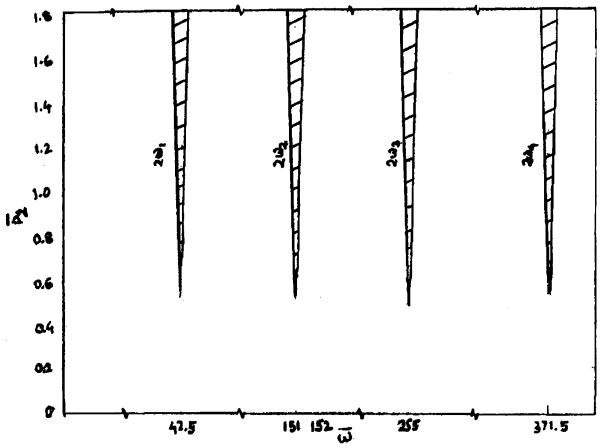

Fig.2.23 (a) Effect of g on zones of instability: g = 10

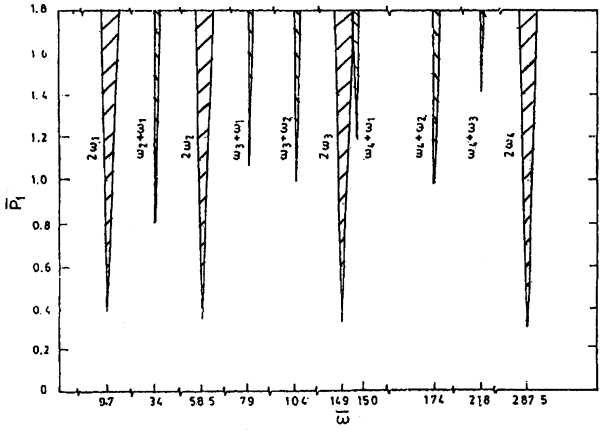

Fig.2.24 (b) Effect of λ_0 on zones of instability: λ_0 = 0.1

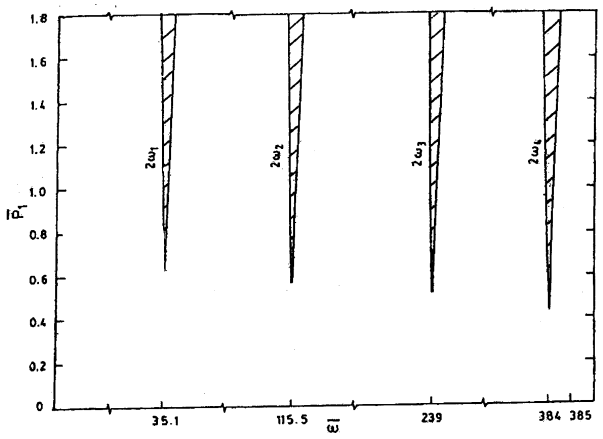

Fig.2.25 (a) Effect of λ_0 on zones of instability: $\lambda_0 = 1.0$

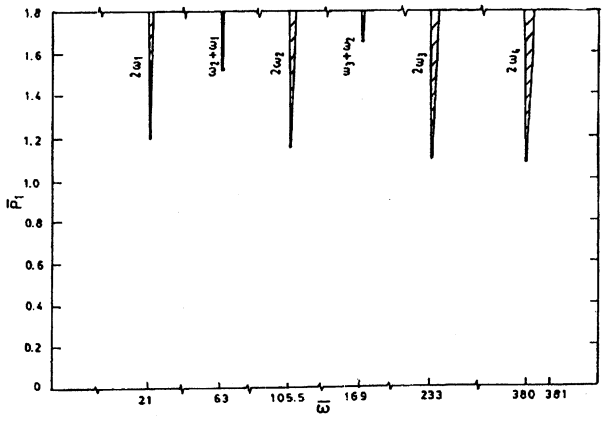

Fig.2.26 (b) Effect of λ_0 on zones of instability: $\lambda_0 = 10.0$

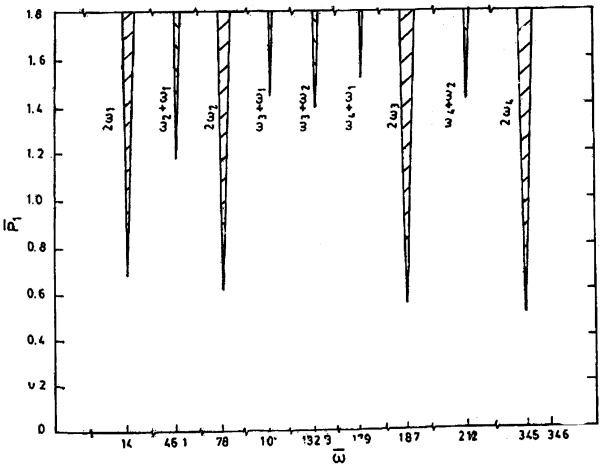

Fig.2.25 (b) Effect of λ_0 on zones of instability: $\lambda_0 = 1.0$

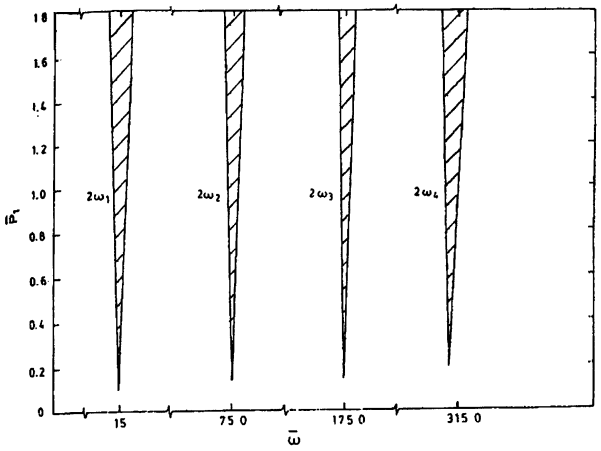

Fig.2.27 (a) Effect of h_{31} on zones of instability: $h_{31} = 2.0$

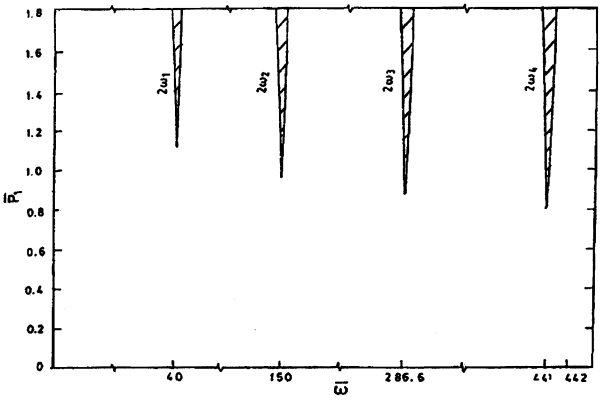

Fig.2.26 (a) Effect of λ_0 on zones of instability: $\lambda_0 = 10.0$

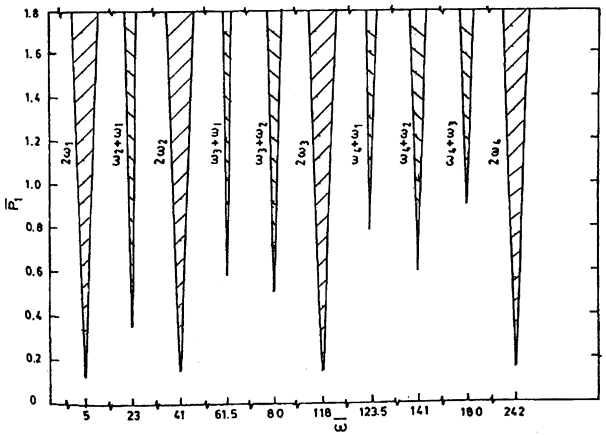

Fig.2.27 (b) Effect of h_{31} on zones of instability: $h_{31} = 2.0$

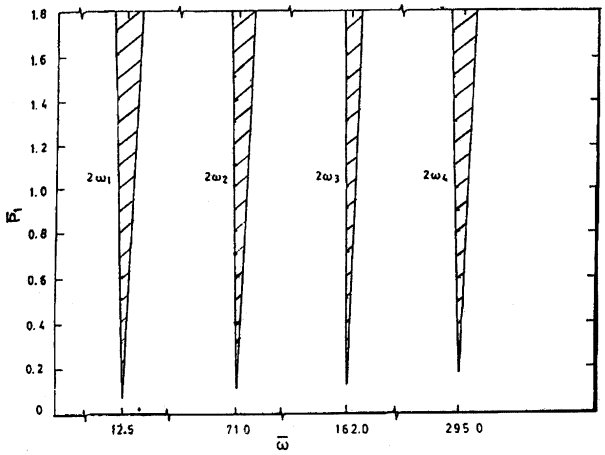

Fig.2.28 (a) Effect of h_{31} on zones of instability: h_{31} = 5.0

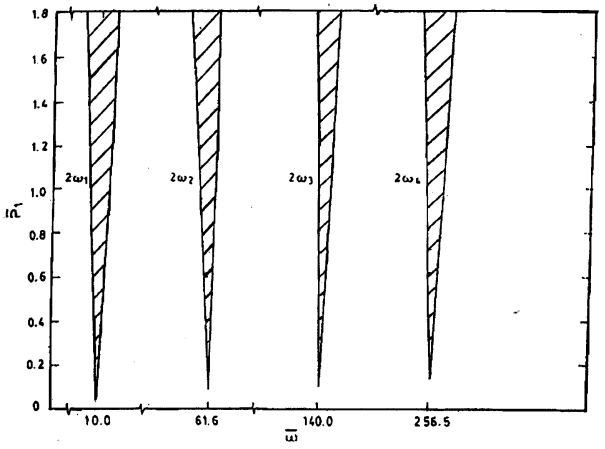

Fig.2.29 (a) Effect of h_{31} on zones of instability: h_{31} = 10

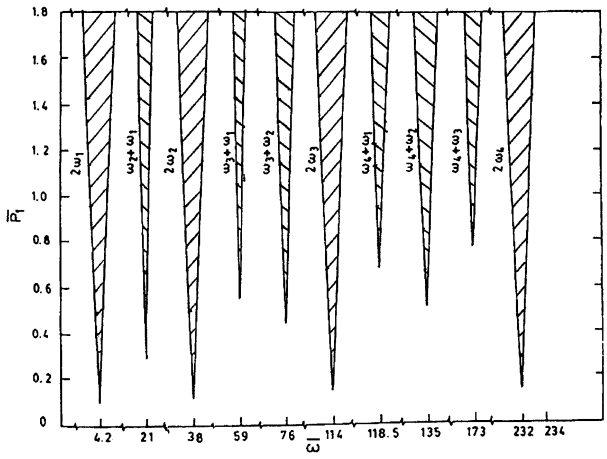

Fig.2.28 (b) Effect of h_{31} on zones of instability: h_{31} = 5.0

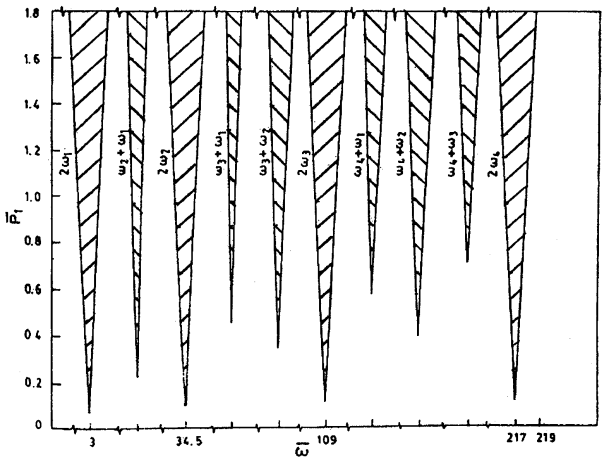

Fig.2.29 (a) Effect of h_{31} on zones of instability: h_{31} = 10

An increase in h_{31} broadens the zones of stability as well as pushes them to the left. Thus, it has a detrimental effect on parametric stability of the system. All this is evident from Figs.2.27(a, b) to Fig. 2.29(a, b).

Conclusions

Stability of the system is improved with the increase of core loss factor. L_{h1}, modulli ratio G_2/E_1, and shear parameter of the core. The stability of the system worsens and improves for low and high values of h_{12} respectively and it worsens as $\bar{b}$ increases. The resonance zones remain almost unaffected for low values of rotation parameter and as it raises above 0.1 the stability deteriorates for pinned-pinned case but for clamped free case, stability worsens near $\omega_2 + \omega_1$, $\omega_3 + \omega_1$ and $\omega_3 + \omega_2$ and improves near $\omega_4 + \omega_1$, $\omega_4 + \omega_2$ and $\omega_4 + \omega_3$ for higher values of $\bar{\omega}$.

In the present work an attempt has been made to include rotation parameter which affects the zones of stability.

References

1. Saito, H. and Otomi, K., "Parametric Response of Viscoelastically Supported Beams", Journal of Sound and Vibration, Vol.63, No. 2, 1979, pp. 169-178.

2. Bauer, H.F. and Eidel, W., "Vibration of Rotating Uniform Beam, Part-II : Orientation Perpendicular to the Axis of Rotation", Journal of Sound Vibration, Vol.122, 1988, p.357.

3. Abbas, B.A.H., "Vibration of Timoshenko Beams with Elasticity Restrained Ends", Journal of Sound and Vibration, Vol.97, 1984, p.541.

4. Leipholz, H., "Stability Theory", Second Edition, John Wiley and Sons, Chichester.

5. Abbas, B.A.H. and Thomas, J., "Dynamic Stability of Timishenko Beams Resting on an Elastic Foundation", Journal of Sound and Vibration, Vol.108, 1986, p.25.

6. Hauchau, O.A. and Hong, C.H., "Nonlinear Response and Stability Analysis of Beams Using Finite Elements in Time", AIAA Journal 26, 1988, p.1135.

7. Kar, R.C. and Sujata, T., "Dynamic Stability of a Rotating Beam with Various Boundary Conditions", Computers and Structures, Vol.40, 1991, p.753.

8. Kar, R.C. and Sujata, T., "Dynamic Stability of a Rotating, Pretwisted and Proconed Cantilever Beam Including Coriolis Effects", Computers and Structures, Vol.42, 1992, p.741.

9. Tan, T.H., Lee, H.P. and Leng, G.S.B., "Parametric Instability of Spinning Pretwisted Beams Subjected to Sinusoidal Compressive Axial Loads", Computers and Structures, Vol.66, 1998, p.745.

10. Kerwin, E.M.Jr., "Damping of Flexural Waves by a Constrained Viscoelastic Layer", The Journal of the Acoustical Society of America, Vol.31, 1959, p.952.

11. Ghosh Ranajay, Dharmvaram Sanjay, Ray Kumar, and Dash, P., "Dynamic Stability of a Viscoelasticity Supported Sandwich Beam", Structural Engineering and Mechanics, Vol.19, No. 5, 2005, pp.503-517.

Annexure

Configuration of a rotating, pretwisted and preconed cantilever beam

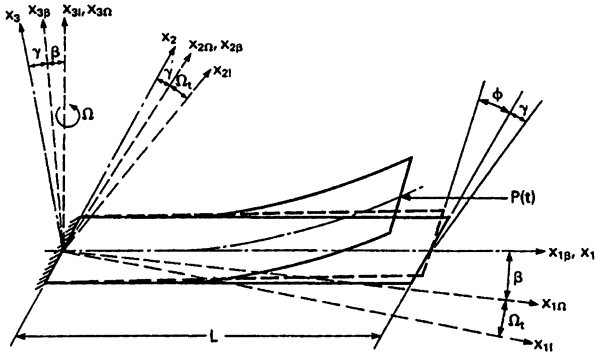

Φ-pretwist angle

β - preconed angle

γ - setting angle